Diversity-Oriented Synthesis as a Strategy for Fragment Evolution against GSK3#

ACS Medicinal Chemistry Letters

Letter

pubs.acs.org/acsmedchemlett

Diversity-Oriented Synthesis as a Strategy for Fragment Evolution against GSK3β

Yikai Wang,[†] Jean-Yves Wach,[†] Patrick Sheehan,[†] Cheng Zhong,[†] Chenyang Zhan,[§] Richard Harris,[§] Steven C. Almo,[§] Joshua Bishop,[†,‡] Stephen J. Haggarty,[†,‡] Alexander Ramek,[†] Kayla N. Berry,[†] Conor O'Herin,[†] Angela N. Koehler,[†] Alvin W. Hung,[*,∥,†] and Damian W. Young[*,⊥,†]

[†]Chemical Biology Program, The Broad Institute of Harvard and MIT, 415 Main Street, Cambridge, Massachusetts 02142, United States

[‡]Department of Neurology & Psychiatry, Harvard Medical School and Massachusetts General Hospital, 185 Cambridge Street, Boston, Massachusetts 02114, United States

[§]Department of Biochemistry, Albert Einstein College of Medicine, 1300 Morris Park Avenue, Bronx, New York 10461, United States

Supporting Information

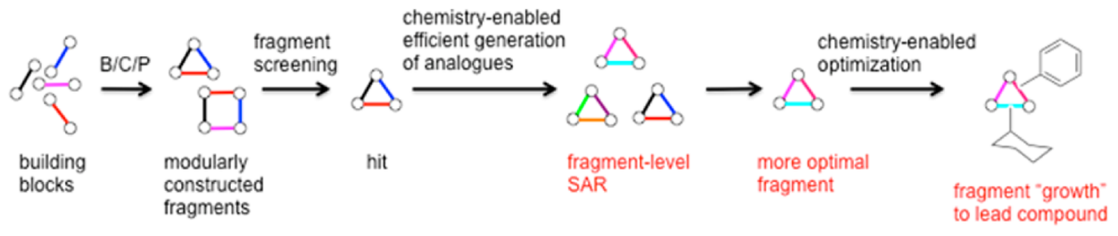

ABSTRACT: Traditional fragment-based drug discovery (FBDD) relies heavily on structural analysis of the hits bound to their targets. Herein, we present a complementary approach based on diversity-oriented synthesis (DOS). A DOS-based fragment collection was able to produce initial hit compounds against the target GSK3β, allow the systematic synthesis of related fragment analogues to explore fragment-level structure−activity relationship, and finally lead to the synthesis of a more potent compound.

KEYWORDS: *Diversity oriented synthesis, fragment-based drug discovery, fragment growing, GSK3β*

Fragment-based drug discovery (FBDD) is an established approach for generating therapeutic lead molecules.[1−4] Key to the optimization process is the application of structure-based methods to guide the synthetic decision-making of growing fragment hits into more potent compounds.[5−8] However, the strong reliance on highly resolved fragment-target structures can be limiting. Targets that do not readily lend themselves to structure-guided approaches provide little recourse to FBDD.[9,10] A strategy for evolving more potent compounds from fragments that does not completely depend on structure-based methods would be a useful tool within the FBDD arena, making the approach more broadly applicable.

There have been recent discussions related to evolving fragment scaffolds without structural guidance. For example, Konrat and co-workers described a strategy for using protein meta-analysis and ligand-based nuclear magnetic resonance (NMR) techniques to generate leads against two targets without 3D structures.[11] Similarly, Viola and co-workers reported a systematic chemistry approach to explore fragment-level structure−activity relationships (SAR).[12] The development of other methods to evolve and optimize fragments[13] without structural guidance would certainly expand the generality of the FBDD approach. Toward this goal, we herein describe the application of diversity-oriented synthesis (DOS) to discover and optimize fragments to the kinase GSK3β.

DOS involves the generation of skeletal, stereochemical, regiochemical, and appendage variations using a common synthesis scheme.[14,15] The build/couple/pair (B/C/P) strategy in DOS was developed to guide, in a modular fashion, the synthetic planning processes to efficiently generate diverse compounds.[16−18] This produces a broader degree of variation in molecular structure in a set of compounds compared to other approaches. Importantly, this molecular diversity is produced under the aegis of one general synthesis pathway, which significantly simplifies the synthetic planning and development throughout the discovery and lead generation phases. The merits of the B/C/P approach have been demonstrated in various high-throughput screening (HTS) applications.[19−21] Here, we extend the concept of DOS toward the application of fragment-based drug discovery (Figure 1).

A small set of 86 fragments was prepared and screened against glycogen synthase kinase 3β (GSK3β), a serine threonine kinase, which is aberrantly overexpressed in cancer

Received: June 4, 2016
Accepted: July 14, 2016
Published: July 14, 2016

DOI: 10.1021/acsmedchemlett.6b00230
ACS Med. Chem. Lett. 2016, 7, 852−856

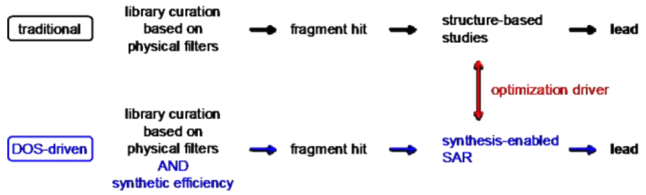

Figure 1. Logical chemical synthesis strategy related to the fragments would impact optimization and modification of fragment hits. Fragments constructed using highly modular syntheses would enable rapid substitutions around a fragment core. Therefore, the generation of fragment-SAR using modular fragment syntheses would aid the fragment evolution process as a complementary approach to structure-guided approaches.

and Alzheimer's disease.[22−25] These fragments were derived from three different pathways[26−28] using the DOS B/C/P approach (Figure 2a). Accordingly the modular synthetic routes could be exploited to generate fragment-level SAR from an identified hit.

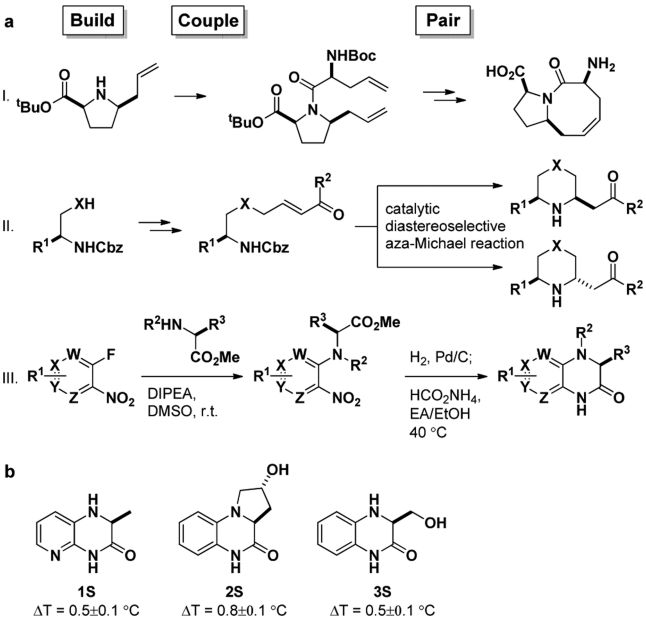

Figure 2. (a) Three different build/couple/pair pathways leading to a library of skeletally and stereochemically diverse fragments. (b) Fragment hits from a DSF screening at 2.5 mM against GSK3β. Compounds displaying a thermal shift ≥0.5 °C are shown.

As shown in Figure 2b, differential scanning fluorimetry (DSF) was used as the primary screening method for detecting fragment binding against GSK3β. Interestingly, three compounds from the same synthetic pathway (pathway **III**) displayed weak thermal stabilization (ΔT) of 0.5 °C or greater (Figure 2b).

The detailed synthesis of **1S** is shown in Figure 3a.[26] Here, the build phase consisted of procuring commercially available arylnitrofluorides and α-amino esters. The appropriate arylnitrofluorides were then coupled with amino esters using S_NAr reactions to yield **1S′**. Subsequent reduction of the nitro group under mild conditions afforded the aniline, which underwent concomitant cyclization (the pairing phase) to the desired product **1S**. The enantiomeric excess of compounds produced by this synthetic pathway was verified by chiral HPLC analysis to be greater than 95% in all cases, allowing for

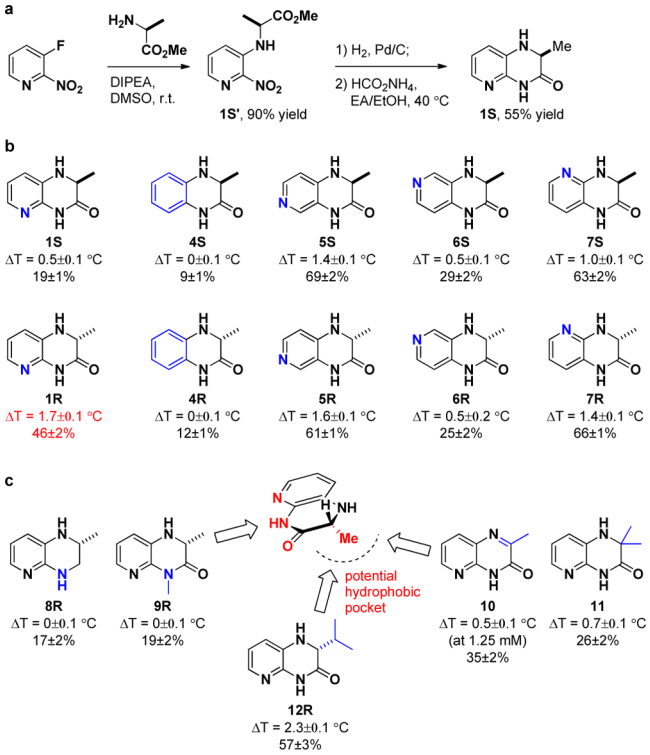

Figure 3. (a) Synthesis of **1S** as a representation of the B/C/P pathway. (b) DSF and biochemical assay results of analogues of **1S**. (c) Chemical modifications on **1R** to identify key binding interactions and probe potential pocket for fragment growing. DSF assays were performed at 2.5 mM unless otherwise indicated; biochemical assays were performed at 1 mM.

activity comparison using compounds with equivalent enantiopurity.

Based on the B/C/P pathway described above, a series of structurally similar compounds to parent fragment **1S** was synthesized and evaluated in DSF experiments. In parallel, using ADP-Glo assays, single-point biochemical inhibitions were also performed to rank compounds based on their inhibition against GSK3β (at 1 mM). As shown in Figure 3b, fragment **1R** (antipode of the initial hit **1S**) showed a larger ΔT and inhibition than the original fragment hit **1S** (1.7 °C and 46% inhibition at 1 mM, Figure 3b). The variation in thermal stabilizations and inhibitions of both fragment enantiomers against GSK3β provided early validation of fragment binding.

Some preliminary structure−activity relationships could also be observed from the set of piperazinone compounds synthesized. Fused pyridyl rings to the piperazinone scaffolds were found to stabilize GSK3β more favorably than their phenyl counterparts. As shown in Figure 3b, both enantiomeric compounds **4S** and **4R** had no measurable effect in the DSF. It was also found that the position of the nitrogen in the pyridyl rings affected the thermal stabilization of GSK3β. Importantly, depending on the position of the pyridine-*N*, the extent of variation in activity and thermal stabilizations of the corresponding enantiomers was different. We hypothesize that these regioisomers bind to GSK3β through nonidentical binding conformations, accounting for differences in stabilization between antipodes. Based on the qualitative DSF and point inhibition results, fragment **1R** was prioritized for further optimization.

DOI: 10.1021/acsmedchemlett.6b00230
ACS Med. Chem. Lett. 2016, 7, 852−856

Pyridinyl amides are known hinge binding motifs against kinases.[29] We postulated that this interaction is also present for fragment **1R** (Figure 3c). This hypothesis was further corroborated with the synthesis of compounds **8R** and **9R**. The deletion of the amide carbonyl in **1R** abolished thermal stabilization of fragment **8R**. Additionally, removal of the hydrogen bond donor capacity by *N*-methylation of the amide nitrogen (compound **9R**) resulted in significantly lower stabilization of GSK3β.

At this stage, saturation transfer difference (STD)[30] and WaterLOGSY[31] NMR experiments were also performed to validate binding of **1R**. As shown in Figure 4, both ligand-based

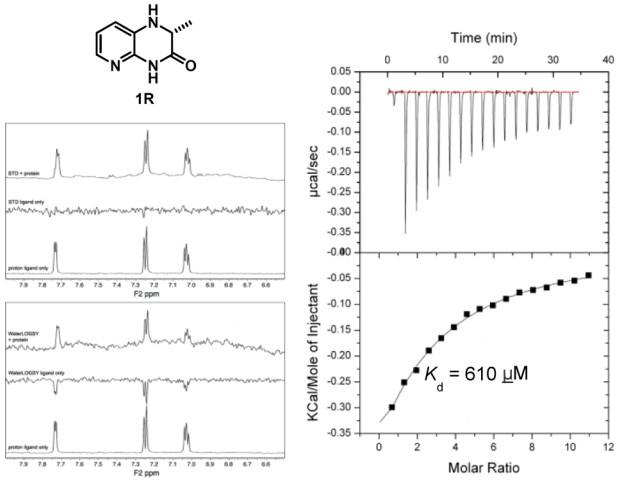

Figure 4. (a) STD NMR spectrum of **1R** against GSK3β. (b) WaterLOGSY NMR spectrum of **1R** against GSK3β. Both NMR techniques further validated binding of fragment **1R** against GSK3β. (c) Using ITC, **1R** was determined to bind against GSK3β with K_d = 610 μM (LE = 0.37).

NMR experiments show compound **1R** binding unambiguously to GSK3β, corroborating thermal shift results. With the results in hand, isothermal titration calorimetry (ITC) was then used to quantitatively evaluate the equilibrium dissociation constant (K_d) of fragment **1R**. Compound **1R** was found to bind to GSK3β with K_d = 0.6 mM with a desirable ligand efficiency (LE) of 0.37 (Figure 4c).

In an effort to evaluate the importance of the chiral center residing in **1R**, three analogues were prepared (Figure 3c). Oxidation of **1R** afforded compound **10**, therefore removing the chirality of **1R**. This planar fragment resulted in diminished activity and low thermal stability as compared to **1R**. Installation of a gem-dimethyl group produced compound **11**, which did not provide thermal shifts equivalent to **1R**. This indicated that the binding pocket cannot easily accommodate two hydrophobic groups on both faces of the fragment. Finally, to probe the size of the binding pocket, a larger isopropyl-containing analogue **12R** was synthesized, which showed a ΔT of 2.3 °C (0.6 °C more stable than **1R**). Given this last observation, we concluded that the chiral center, in particular with the *R* configuration, was a potential growth vector to increase potency. Therefore, from the fragment SAR generated at this point, we were equipped with a rational plan to evolve the fragment into a more potent compound.

The B/C/P pathway was once again utilized to generate analogues of **1R** with larger groups from the corresponding amino ester starting materials (optimization phase). Both enantiomers were synthesized to provide side-by-side comparisons of the two stereogenic growth vectors. DSF and single-point inhibition assays were used to evaluate their binding interaction and inhibitory activity, respectively.

As shown in Figure 5, the binding of larger aromatic groups was accommodated in GSK3β similarly to aliphatic groups in

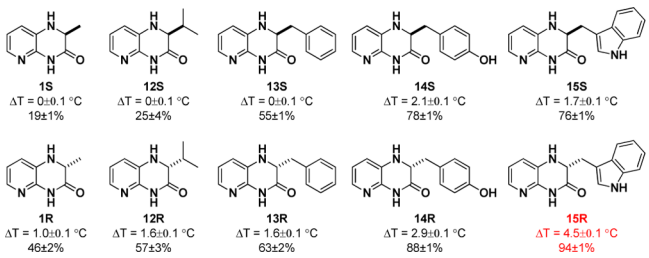

Figure 5. Small set of compounds were synthesized, extending from a growth vector identified from previous SAR. For ranking purposes, DSF assays were performed at 1.25 mM for comparison, and point inhibition biochemical assays were performed at 1 mM.

compounds **1R** and **12R**. Interestingly, an additional hydroxyl group on the phenyl ring (compound **14R**) led to a significant increase in potency, leading us to surmise that a larger, electron-rich aromatic group could be tolerated. Satisfyingly, compound **15R** with an indolyl substitution resulted in a 4.5 °C thermal stabilization when tested at 1.25 mM. Results from the biochemical assay conducted at a single concentration (1 mM) correlated well with the DSF results.

Finally, ITC was used to quantify the binding of **15R**, the compound that displayed the greatest thermal stabilization against GSK3β. As shown in Figure 6a, compound **15R** bound to GSK3β with K_d = 9 μM, a greater than 60-fold improvement in binding over **1R**. Additionally, **15R** was found to inhibit GSK3β with an IC_{50} = 18 μM. The enantiomer **15S** was also tested and was ~18-fold less active than **15R** (IC_{50} = 322 μM,

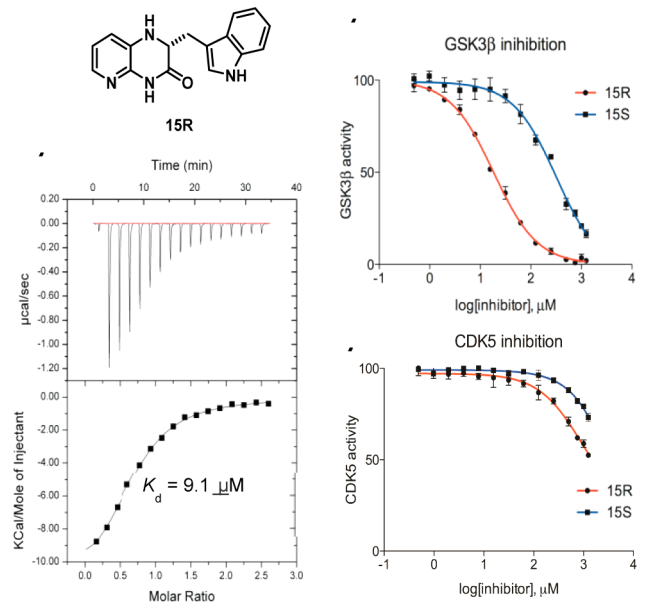

Figure 6. (a) ITC K_d determination of **15R** against GSK3β K_d = 9.1 μM. (b) Biochemical inhibition measurements of **15R** (IC_{50} = 18 μM) and **15S** (IC_{50} = 322 μM) against GSK3β. (c) IC_{50} measurement of **15R** and **15S** against CDK.

DOI: 10.1021/acsmedchemlett.6b00230
ACS Med. Chem. Lett. 2016, 7, 852−856

Figure 6b), a result that is reflected by the low thermal shifts observed by DSF.

As shown in Figure 6c, **15R** demonstrates 50-fold selectivity against GSK3β over the closely related kinase Cyclin-dependent Kinase 5 (CDK5). The selectivity profile of the chiral compound **15R** against GSK3β over CDK5 is an attractive starting point for the preparation of additional ligands with more enhanced selectivity toward GSK3β. It is also noteworthy that compound **15R** has a low molecular weight of 278 g/mol (LE of 0.33) and provides further synthetic growth opportunities toward achieving greater potency.

In most FBDD efforts, X-ray analysis is performed at the earliest stage to guide optimization chemistry. However, it was our goal to demonstrate that the modular B/C/P chemistry alone would be advantageous toward optimizing a fragment hit. To corroborate the fragment growing approach, X-ray crystal structures of GSK3β in complex with **1R** and **15R** were determined.

Consistent with our SAR analysis, **1R** and **15R** were found to occupy the ATP-binding site, which is at the interface between the N-terminal β-strand domain and C-terminal α-helix domain[32,33] (see Supporting Information Figure S4). Most interactions with **15R** are contributed by the hinge region (D133-T138) of GSK3β (Figure 7). The amide NH of **15R**

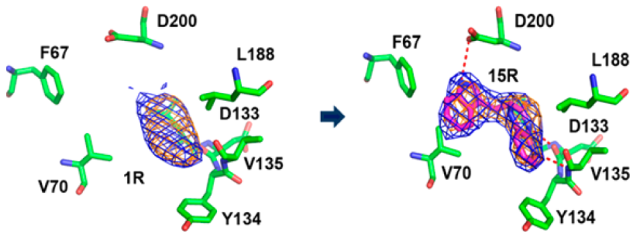

Figure 7. X-ray crystal structure of **1R** and **15R** against GSK3β. The $2F_o$-F_c (1σ) and F_o-F_c maps (3σ) around **15R** are shown as blue and orange meshes, respectively. Polar interactions are displayed as red dashed lines. PDB ID for **1R**, 4J71; for **15R**, 4J1R.

makes a hydrogen bond with the backbone oxygen of D133. The pyridyl nitrogen forms an additional hydrogen bond with the backbone NH of V135. The structural results were consistent with our synthetically obtained SAR studies. More interestingly, the indole substituent is found to be off-plane to the hinge binding region. As a result, multiple hydrophobic interactions with residues F67 and V70 are formed, contributing to the ~60-fold improvement in binding potency over the initial fragment. There is also possibility of hydrogen bond or salt bridge formation between the indole nitrogen on **15R** and the side chain of D200. However, the distance between these two atoms is 3.4 Å, suggesting the interaction to be weak. In contrast, the *S* enantiomer failed to provide these interactions in a stereochemically matched manner, leading to diminished affinity.

The X-ray crystal structure of the fragment hit **1R** occupied the same site as **15R** (Figure 7). However, due to modest resolution, an unambiguous placement of **1R** in the electron density was not possible. Multiple binding modes are commonly encountered in the X-ray analysis of fragments to targets given that they may contain other energetically similar weak binding poses. Guided by SAR, our strategy enabled us to generate analogues of **1R** in a systematic fashion to produce a more potent compound when a highly definitive placement of the initial fragment hit within the binding pocket could not be determined. Although X-ray did not guide our chemical optimizations, we envision that our approach will also be useful with an X-ray structure of the fragment−ligand complex since the modular B/C/P chemistry can be used to prepare specific analogues suggested from the structure.

In conclusion, a set of novel fragments was generated using a DOS-driven B/C/P approach. This set of compounds was screened against GSK3β, and from the screen the pyridyl piperazinone fragment hit **1R** (K_d = 0.6 mM) was identified. It is noteworthy that the stereoselective binding preference of a particular antipode of the piperazinone ring lends toward validation of fragment binding. More importantly, the modular synthesis allows access to different analogues of the fragment hit, enabling quick SAR determination around the fragment. Consequently, fragment growing was exploited through the chiral center of **1R** leading to a more potent binder **15R** (K_d = 9.1 μM). Finally, both **1R** and **15R** were soaked against GSK3β, and the X-ray crystal structure revealed a successful fragment growing approach.

Based on the work described here, we contend that a modular diversity-oriented synthetic approach toward designing fragments is warranted. The ability to efficiently control the modification of a fragment core would greatly assist fragment-level SAR. This in turn expedites structure-guided FBDD and more crucially provides a way of fragment evolution when no target-fragment structural information is available.

■ ASSOCIATED CONTENT

Supporting Information

The Supporting Information is available free of charge on the ACS Publications website at DOI: 10.1021/acsmedchemlett.6b00230.

Chemical structures and PMI analysis of DOS fragments, detailed synthesis and characterization of compounds **1** to **15**, DSF, biochemical assays, NMR spectroscopy, isothermal titration calorimetry, and crystallography studies (PDF)

■ AUTHOR INFORMATION

Corresponding Authors

*E-mail: damiany@bcm.edu.
*E-mail: whung@etc.a-star.edu.sg.

Present Addresses

[‖]Experimental Therapeutics Centre (A-STAR), 11 Biopolis Way #03-10, Singapore 138667.
[⊥]Center for Drug Discovery, Baylor College of Medicine, One Baylor Plaza, Houston, Texas 77030, United States.

Funding

Funding support was provided by Broad Institute SPARC Grant. Additional support for the Haggarty Laboratory was provided by the NIH/NIMH (R01MH091115), the Tau Consortium, and the Barrus Foundation. Additional support for the Almo Laboratory was provided by by NIH/NIGMS U54 GM094662 and NIH/NCI P30 CA013330.

Notes

The authors declare no competing financial interest.

DOI: 10.1021/acsmedchemlett.6b00230
ACS Med. Chem. Lett. 2016, 7, 852−856

■ ACKNOWLEDGMENTS

We acknowledge Dr. Errol L. Samuel for helpful discussions and review of this manuscript. We acknowledge Dr. Yury Patskovsky for his contribution in crystallography modeling.

■ DEDICATION

This work is dedicated to Professor Stuart L. Schreiber on the occasion of his 60th birthday

■ REFERENCES

(1) Chessari, G.; Woodhead, A. J. Recent developments in fragment-based drug discovery. *Drug Discovery Today* **2009**, *14*, 668−675.
(2) Congreve, M.; Chessari, G.; Tisi, D.; Woodhead, A. J. Recent developments in fragment-based drug discovery. *J. Med. Chem.* **2008**, *51*, 3661−3680.
(3) Murray, C. W.; Rees, D. C. The rise of fragment-based drug discovery. *Nat. Chem.* **2009**, *1*, 187−192.
(4) van Montfort, R. L. M.; Collins, I. Fragment-Based Methods in Drug Discovery: It's the Small Things that Matter. *Curr. Top. Med. Chem.* **2009**, *9*, 1676−1677.
(5) Blundell, T. L.; Jhoti, H.; Abell, C. High-throughput crystallography for lead discovery in drug design. *Nat. Rev. Drug Discovery* **2002**, *1*, 45−54.
(6) Ciulli, A.; Abell, C. Fragment-based approaches to enzyme inhibition. *Curr. Opin. Biotechnol.* **2007**, *18*, 489−496.
(7) Hennig, M.; Ruf, A.; Huber, W. Combining biophysical screening and X-ray crystallography for fragment-based drug discovery. *Top. Curr. Chem.* **2011**, *317*, 115−143.
(8) Jhoti, H.; Cleasby, A.; Verdonk, M.; Williams, G. Fragment-based screening using X-ray crystallography and NMR spectroscopy. *Curr. Opin. Chem. Biol.* **2007**, *11*, 485−493.
(9) Granseth, E.; Seppala, S.; Rapp, M.; Daley, D. O.; Von Heijne, G. Membrane protein structural biology - How far can the bugs take us? *Mol. Membr. Biol.* **2007**, *24*, 329−U323.
(10) Torres, J.; Stevens, T. J.; Samso, M. Membrane proteins: the 'Wild West' of structural biology. *Trends Biochem. Sci.* **2003**, *28*, 137−144.
(11) Henen, M. A.; Coudevylle, N.; Geist, L.; Konrat, R. Toward Rational Fragment-Based Lead Design without 3D Structures. *J. Med. Chem.* **2012**, *55*, 7909−7919.
(12) Thangavelu, B.; Bhansali, P.; Viola, R. E. Elaboration of a Fragment Library Hit Produces Potent and Selective Aspartate semialdehyde Dehydrogenase Inhibitors. *Bioorg. Med. Chem.* **2015**, *23*, 6622−6631.
(13) Hung, A. W.; Silvestre, H. L.; Wen, S.; George, G. P.; Boland, J.; Blundell, T. L.; Ciulli, A.; Abell, C. Optimization of inhibitors of Mycobacterium tuberculosis Pantothenate Synthetase based on group efficiency analysis. *ChemMedChem* **2016**, *5*, 38−42.
(14) Burke, M. D.; Schreiber, S. L. A planning strategy for diversity-oriented synthesis. *Angew. Chem., Int. Ed.* **2004**, *43*, 46−58.
(15) Schreiber, S. L. Target-oriented and diversity-oriented organic synthesis in drug discovery. *Science* **2000**, *287*, 1964−1969.
(16) Nielsen, T. E.; Schreiber, S. L. Diversity-oriented synthesis - Towards the optimal screening collection: A synthesis strategy. *Angew. Chem., Int. Ed.* **2008**, *47*, 48−56.
(17) Spiegel, D. A.; Schroeder, F. C.; Duvall, J. R.; Schreiber, S. L. An oligomer-based approach to skeletal diversity in small-molecule synthesis. *J. Am. Chem. Soc.* **2006**, *128*, 14766−14767.
(18) Dandapani, S.; Marcaurelle, L. A. Current strategies for diversity-oriented synthesis. *Curr. Opin. Chem. Biol.* **2010**, *14*, 362−370.
(19) Marcaurelle, L. A.; Comer, E.; Dandapani, S.; Duvall, J. R.; Gerard, B.; Kesavan, S.; Lee, M. D.; Liu, H. B.; Lowe, J. T.; Marie, J. C.; Mulrooney, C. A.; Pandya, B. A.; Rowley, A.; Ryba, T. D.; Suh, B. C.; Wei, J. Q.; Young, D. W.; Akella, L. B.; Ross, N. T.; Zhang, Y. L.; Fass, D. M.; Reis, S. A.; Zhao, W. N.; Haggarty, S. J.; Palmer, M.; Foley, M. A. An Aldol-Based Build/Couple/Pair Strategy for the Synthesis of Medium- and Large-Sized Rings: Discovery of Macrocyclic Histone Deacetylase Inhibitors. *J. Am. Chem. Soc.* **2010**, *132*, 16962−16976.
(20) Peng, L. F.; Stanton, B. Z.; Maloof, N.; Wang, X.; Schreiber, S. L. Syntheses of aminoalcohol-derived macrocycles leading to a small-molecule binder to and inhibitor of Sonic Hedgehog. *Bioorg. Med. Chem. Lett.* **2009**, *19*, 6319−6325.
(21) Stanton, B. Z.; Peng, L. F.; Maloof, N.; Nakai, K.; Wang, X.; Duffner, J. L.; Taveras, K. M.; Hyman, J. M.; Lee, S. W.; Koehler, A. N.; Chen, J. K.; Fox, J. L.; Mandinova, A.; Schreiber, S. L. A small molecule that binds Hedgehog and blocks its signaling in human cells. *Nat. Chem. Biol.* **2009**, *5*, 154−156.
(22) Hanger, D. P.; Anderton, B. H.; Noble, W. Tau phosphorylation: the therapeutic challenge for neurodegenerative disease. *Trends Mol. Med.* **2009**, *15*, 112−119.
(23) Hernandez, F.; Lucas, J. J.; Avila, J. GSK3 and Tau: Two Convergence Points in Alzheimer's Disease. *J. Alzheimers Dis.* **2013**, *33*, S141−144.
(24) Hoeflich, K. P.; Luo, J.; Rubie, E. A.; Tsao, M. S.; Jin, O.; Woodgett, J. R. Requirement for glycogen synthase kinase-3 beta in cell survival and NF-kappa B activation. *Nature* **2000**, *406*, 86−90.
(25) Luo, J. Glycogen synthase kinase 3 beta (GSK3 beta) in tumorigenesis and cancer chemotherapy. *Cancer Lett.* **2009**, *273*, 194−200.
(26) Chen, J. J.; Qian, W. Y.; Biswas, K.; Viswanadhan, V. N.; Askew, B. C.; Hitchcock, S.; Hungate, R. W.; Arik, L.; Johnson, E. Discovery of dihydroquinoxalinone acetamides containing bicyclic amines as potent Bradykinin B1 receptor antagonists. *Bioorg. Med. Chem. Lett.* **2008**, *18*, 4477−4481.
(27) Hung, A. W.; Ramek, A.; Wang, Y.; Kaya, T.; Wilson, J. A.; Clemons, P. A.; Young, D. W. Route to three-dimensional fragments using diversity-oriented synthesis. *Proc. Natl. Acad. Sci. U. S. A.* **2011**, *108*, 6799−6804.
(28) Zhong, C.; Wang, Y.; Hung, A. W.; Schreiber, S. L.; Young, D. W. Diastereoselective control of intramolecular aza-Michael reactions using achiral catalysts. *Org. Lett.* **2011**, *13*, 5556−5559.
(29) Gould, A. E.; Adams, R.; Adhikari, S.; Aertgeerts, K.; Afroze, R.; Blackburn, C.; Calderwood, E. F.; Chau, R.; Chouitar, J.; Duffey, M. O.; England, D. B.; Farrer, C.; Forsyth, N.; Garcia, K.; Gaulin, J.; Greenspan, P. D.; Guo, R. B.; Harrison, S. J.; Huan, S. C.; Iartchouk, N.; Janowick, D.; Kim, M. S.; Kulkarni, B.; Langston, S. P.; Liu, J. X.; Ma, L. T.; Menon, S.; Mizutani, H.; Paske, E.; Renou, C. C.; Rezaei, M.; Rowland, R. S.; Sintchak, M. D.; Smith, M. D.; Stroud, S. G.; Tregay, M.; Tian, Y. A.; Veiby, O. P.; Vos, T. J.; Vyskocil, S.; Williams, J.; Xu, T. L.; Yang, J. J.; Yano, J.; Zeng, H. B.; Zhang, D. M.; Zhang, Q.; Galvin, K. M. Design and Optimization of Potent and Orally Bioavailable Tetrahydronaphthalene Raf Inhibitors. *J. Med. Chem.* **2011**, *54*, 1836−1846.
(30) Mayer, M.; Meyer, B. Characterization of Ligand Binding by Saturation Transfer Difference NMR Spectroscopy. *Angew. Chem., Int. Ed.* **1999**, *38*, 1784−1788.
(31) Dalvit, C.; Fogliatto, G.; Stewart, A.; Veronesi, M.; Stockman, B. WaterLOGSY as a method for primary NMR screening: Practical aspects and range of applicability. *J. Biomol. NMR* **2001**, *21*, 349−359.
(32) Bax, B.; Carter, P. S.; Lewis, C.; Guy, A. R.; Bridges, A.; Tanner, R.; Pettman, G.; Mannix, C.; Culbert, A. A.; Brown, M. J. B.; Smith, D. G.; Reith, A. D. The structure of phosphorylated GSK-3 beta complexed with a peptide, FRATtide, that inhibits beta-catenin phosphorylation. *Structure* **2001**, *9*, 1143−1152.
(33) ter Haar, E.; Coll, J. T.; Austen, D. A.; Hsiao, H. M.; Swenson, L.; Jain, J. Structure of GSK3 beta reveals a primed phosphorylation mechanism. *Nat. Struct. Biol.* **2001**, *8*, 593−596.

DOI: 10.1021/acsmedchemlett.6b00230
ACS Med. Chem. Lett. 2016, 7, 852−856